Komiya, K., Soga, K., Akagi, H., Jafari, M. R. & Bolton, M. D. (2001). *Géotechnique* **51**, No. 10, 835–846

# Soil consolidation associated with grouting during shield tunnelling in soft clayey ground

K. KOMIYA,* K. SOGA,† H. AKAGI,‡ M. R. JAFARI§ and M. D. BOLTON†

**The effectiveness of grouting to reduce surface settlements during underground construction in clayey ground was investigated by a field trial and laboratory tests. The field trial was carried out during shield tunnelling work conducted in alluvial clay deposits in Koto-ku, Tokyo. Grout was injected at some distance away from the tunnel, and both surface and subsurface settlements above the tunnel were monitored. Although the initial heave was achieved immediately after the grout injection, the ground continued to settle with time, owing to soil consolidation and grout shrinkage. A laboratory investigation was conducted to investigate the parameters that control the long-term behaviour of grouting in clay. It was found that better long-term grout efficiency can be achieved in overconsolidated clay than in normally consolidated clay, and the efficiency increased with increasing injection volume. Finite element analysis of the laboratory experiments confirmed that the amount and extent of excess pore pressures generated during injection govern the long-term grout efficiency. Finite element analysis of the field trial was also performed to simulate the long-term ground deformation after grout injection.**

**KEYWORDS: clays; consolidation; grouting; laboratory tests; numerical modelling and analysis; tunnels.**

**Nous étudions l'efficacité de la cimentation pour réduire le tassement de surface pendant les constructions souterraines dans des sols argileux au moyen d'essais sur le terrain et d'essais en laboratoire. Les essais sur le terrain ont été faits pendant des travaux de perçage de tunnels protecteurs effectués dans les dépôts d'argile alluviale de Koto-ku à Tokyo. Le ciment a été injecté à une certaine distance du tunnel et les tassements de surface et de sous-surface au-dessus du tunnel ont été observés. Bien que le gonflement initial se soit produit immédiatement après l'injection de ciment, le sol a continué à se tasser peu à peu en raison de sa consolidation et de la contraction du ciment. Une investigation en laboratoire a été menée pour trouver les paramètres qui commandent le comportement à long terme de la cimentation dans l'argile. On a trouvé que l'efficacité à long terme du ciment est meilleure dans une argile surconsolidée que dans une argile à consolidation normale et que l'efficacité augmentait en même temps avec le volume injecté. L'analyse d'éléments finis pratiquée sur les essais en laboratoire a confirmé que l'importance et l'étendue des pressions interstitielles excessives produites pendant l'injection gouvernent l'efficacité à long terme du ciment. Nous avons fait également des analyses d'éléments finis pour l'essai sur le terrain afin de simuler la déformation à long terme du sol après l'injection de ciment.**

## INTRODUCTION

The shield tunnelling method is frequently applied for constructing underground structures for railways and utility lines in urban areas. The method has been used extensively for more than 30 years, and many advances—such as the development of new excavation machines and the implementation of computer-controlled operation—have been made in order to optimise the method. Based on the large amount of experience and expertise, the sources of ground deformation associated with shield tunnelling are well investigated and widely reported (e.g. Mair & Taylor, 1997). In recent years, the magnitude of soil deformation by earth pressure balance shield tunnelling in soft ground has become remarkably small; surface settlements of less than 10 mm are common (e.g. JSSMFE, 1993).

Even with recent advances in the method, shield tunnelling in soft clayey ground, where the SPT N value is close to zero, is still a major technical challenge for tunnel engineers. Deformation in this type of ground tends to occur several months or years after the completion of tunnelling, as shown by the typical time–settlement curve in Fig. 1. This long-term settlement is due mainly to consolidation of clayey soil around the tunnel, originating from the excess pore water pressure generated during the shield tunnelling work as the ground is sheared and disturbed (e.g. Clough *et al.*, 1983; Shirlaw, 1995). Drainage into the tunnel can reduce pore pressures below their original values, and also contributes to the long-term settlement.

Manuscript received 31 January 2000; revised manuscript accepted 10 August 2001.
Discussion on this paper closes 1 May 2002, For further details see inside back cover.
* Department of Civil Engineering, Chiba Institute of Technology, Japan.
† Engineering Department, University of Cambridge, UK.
‡ Department of Civil Engineering, Waseda University, Japan.
§ Massachusetts Institute of Technology, USA.

During shield tunnelling in soft ground, grout materials can be injected around the upper part of tunnel linings to improve the strength of the soil and to reduce the magnitude of surface settlements. In recent years, compensation grouting and grout jacking have been applied successfully in many major tunnelling projects to limit ground settlements under important structures. In this operation, grout is injected at locations between the tunnel and the building foundations in order to 'compensate' for stress relief and ground loss induced by tunnel excavation. In compensation grouting, grout injection is often performed at the same time as tunnel construction (as shown by the shaded zone in Fig. 1), so that building settlements are maintained within the specified criteria. Successful applications of compensation grouting in stiff London clay have been reported for the underground construction of the Jubilee Line Extension Project (Harris *et al.*, 1996; Osborne *et al.*, 1997; Harris *et al.*, 1999). However, its effectiveness in soft clayey soils is still in question (Shirlaw *et al.*, 1999; Soga *et al.*, 1999).

In this study, grout injection tests were performed in the laboratory and in the field to investigate the short- and long-term deformations of clay around grout injection points. Finite element modelling of the laboratory grouting tests was conducted, and the parameters controlling the long-term behaviour of grouting in clay were investigated. Finite element analysis was also performed to simulate the field trial, where grout was injected in soft clayey ground at a shield tunnelling site in Tokyo. Based on the comparison between the numerical results and the laboratory/field data, soil consolidation associated with grouting is discussed in this paper.

## CONCEPTUAL MODELLING OF GROUTING IN CLAYEY SOILS

The mechanism of soil–grout interaction during grout injection is a very complicated one. However, a simple conceptual model, which covers the main features of grouting process in clay, is proposed for the discussion in this paper.

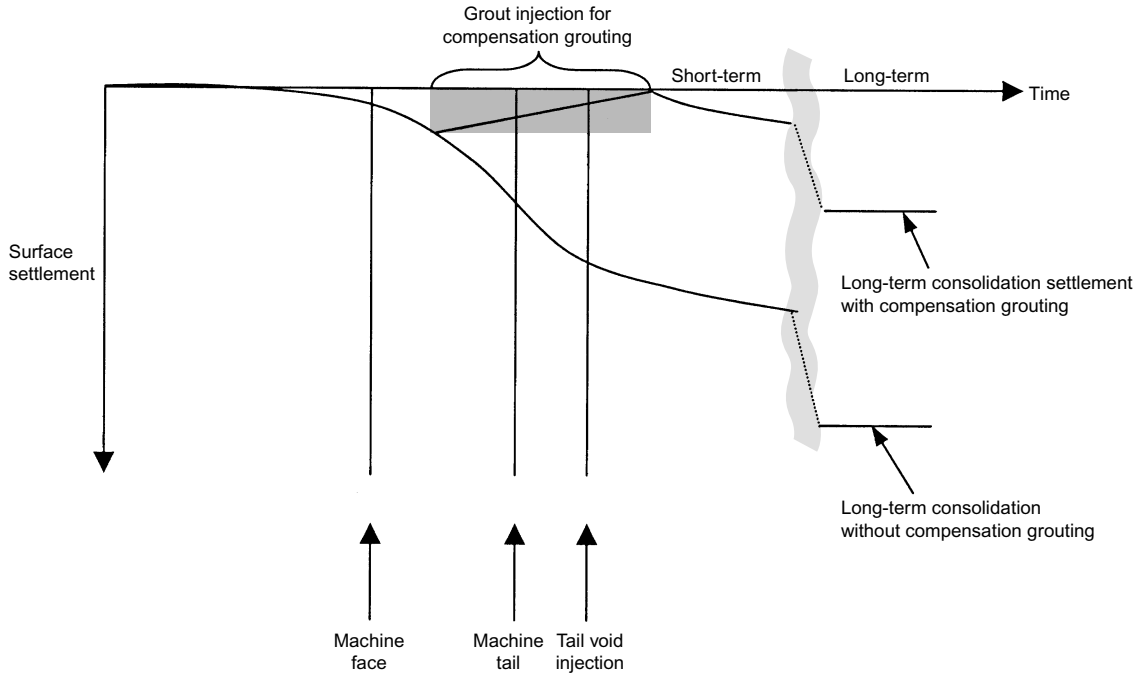


**Fig. 1. Settlements associated with shield tunnelling and compensation grouting**

Grouting can mainly be carried out in two different modes: (*a*) compaction grouting and (*b*) fracture grouting. Compaction grouting involves the injection of high-viscosity stiff grout (e.g. a soil–cement–water mix) into the soil mass. When this type of grout is injected, it does not penetrate into the soil pores but remains in a homogeneous mass, forming an approximately spherical bulb. The formation of a bulb displaces the surrounding soil. Fracture grouting involves the injection of lower-viscosity grout (e.g. cement and bentonite), which tends to result in a split opening the ground (often described as hydraulic fracturing). As the grout flows into the fractures, the surrounding soil is displaced. Hydraulic fracturing can happen even in compaction grouting, which results in loss of control of the grouting process. The shape of a grout body and the subsequent soil fracturing are affected by various parameters such as injection pressure, injection rate, gel time of the grout, rheology of the grout, confining pressure and permeability of the soil (e.g. Mori *et al.*, 1990, 1992; Warner, 1992, 1998).

At the initial stage of grouting, the grout pushes the soil outwards and forms a bulb, as shown in the schematic diagram of Fig. 2(a). As more grout is injected, the clay deforms plastically and the size of the grout bulb grows. It increases until the grout pressure builds up to the fracturing pressure and a plane of weakness is formed by hydraulic fracturing, as shown in Fig. 2(b). Fracture can also occur along a natural fissure, joint or bedding. As fracture occurs, the stress condition in the soil suddenly changes and the injection pressure drops. When lower-viscosity grout is used, the grout will intrude more readily into planes of weakness to form fracture grouting (Fig. 2(c)). When higher-viscosity grout is used, the grout may not able to get into planes of weakness (Fig. 2(c)). The grout bulb continues to expand, and the injection pressure starts to rise again.

The effectiveness of compensation grouting/grout jacking is often evaluated by the amount of soil heave obtained for a given injected grout volume. Ideally, if soil deformation is occurring in the undrained condition, the heave volume is equal

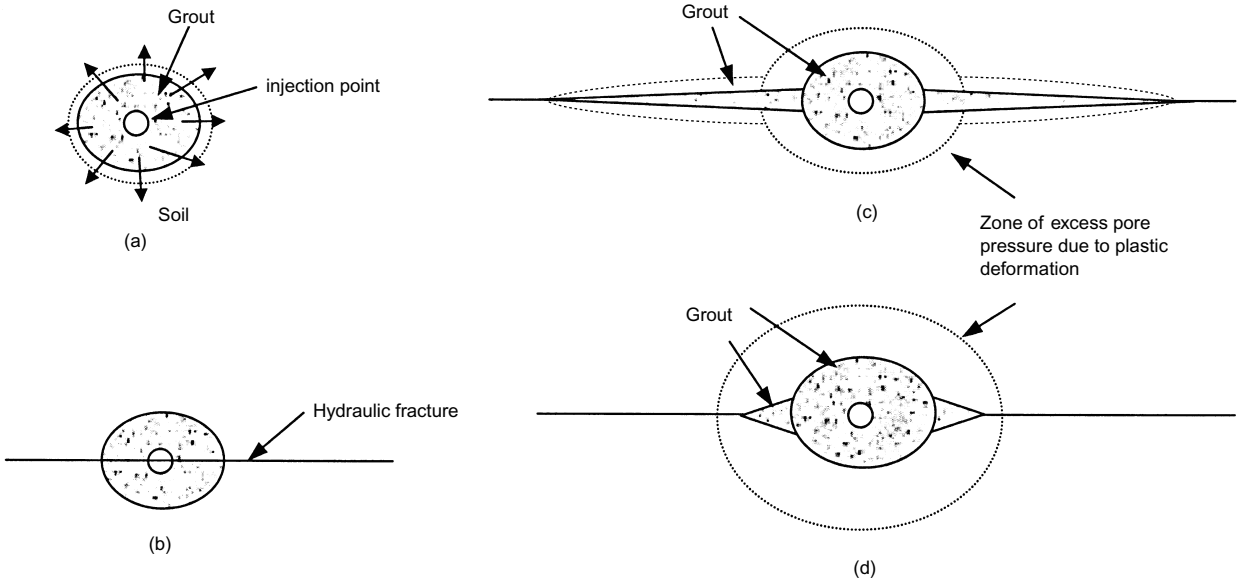


**Fig. 2. Conceptual modelling of grouting in clay: (a) initial stage of grout injection; (b) initiation of fracture; (c) penetration of grout into fracture, low-viscosity grout; (d) penetration of grout into fracture, high-viscosity grout**

to the injection volume. However, this is often not the case in the field, since there will be increased deformation towards the excavation and lateral subsurface displacements leading to surface heave outside the designed compensation area. Therefore injection needs to be controlled by careful monitoring of the surface deformation, so that the overall surface settlements become close to zero after tunnel construction.

Although compensation grouting and grout jacking can be an effective way to reduce surface settlements in the short term, their long-term effectiveness is still not very well known. It is likely that the clay around the grout will consolidate with time, owing to dissipation of the excess pore pressures generated during the injection (Fig. 2(c), (d)). This is especially the case for normally consolidated clays. In addition, the free water in the grout can bleed out from the designed compensation area. If lower-viscosity grout is used, it is possible that the grout escapes from the designed area through the fractures made during injection.

## FIELD INVESTIGATION OF GROUTING IN ALLUVIAL CLAY

### *Field trial*

A field trial of grout jacking was performed during shield tunnelling work conducted in alluvial clay deposits at Koto-ku, Tokyo. A tunnel 3 m diameter and 670 m long was constructed at a depth of 14·3 m using an earth pressure balance shield machine. The soil profile and the location of the tunnel are shown in Fig. 3. The thickness of the clay was approximately 30 m, and the SPT N value is reported to be close to zero throughout the layer. Some physical properties of the soils are listed in Table 1. The clay is normally consolidated with a liquidity index close to 1, and is a typical alluvial clay in Tokyo. Because of the high sensitivity values, large compressibility due to soil structure degradation can result in large long-term settlement, as discussed by Mori & Akagi (1985).

The grout injection trial was performed at three different locations, as shown in Fig. 4. In case A, mortar was injected into the gap between the tunnel lining and the excavated ground (tail void) immediately after the machine passage and installation of tunnel linings. Grout pipes were installed at the tail of the shield machine, and injection was performed when a segmental lining came out from the machine. The injected volume was approximately 120–150% of the theoretical tail void volume, and the injection pressure recorded at the invert was 300 kPa.

Instead of performing tail void grouting, grout jacking was performed above the tunnel by installing five injection pipes from the tunnel (cases B and C in Fig. 4(a)). The effectiveness was examined by injecting grout at two different distances from the tunnel: 1·0 m and 2·0 m in cases B and C respectively (see

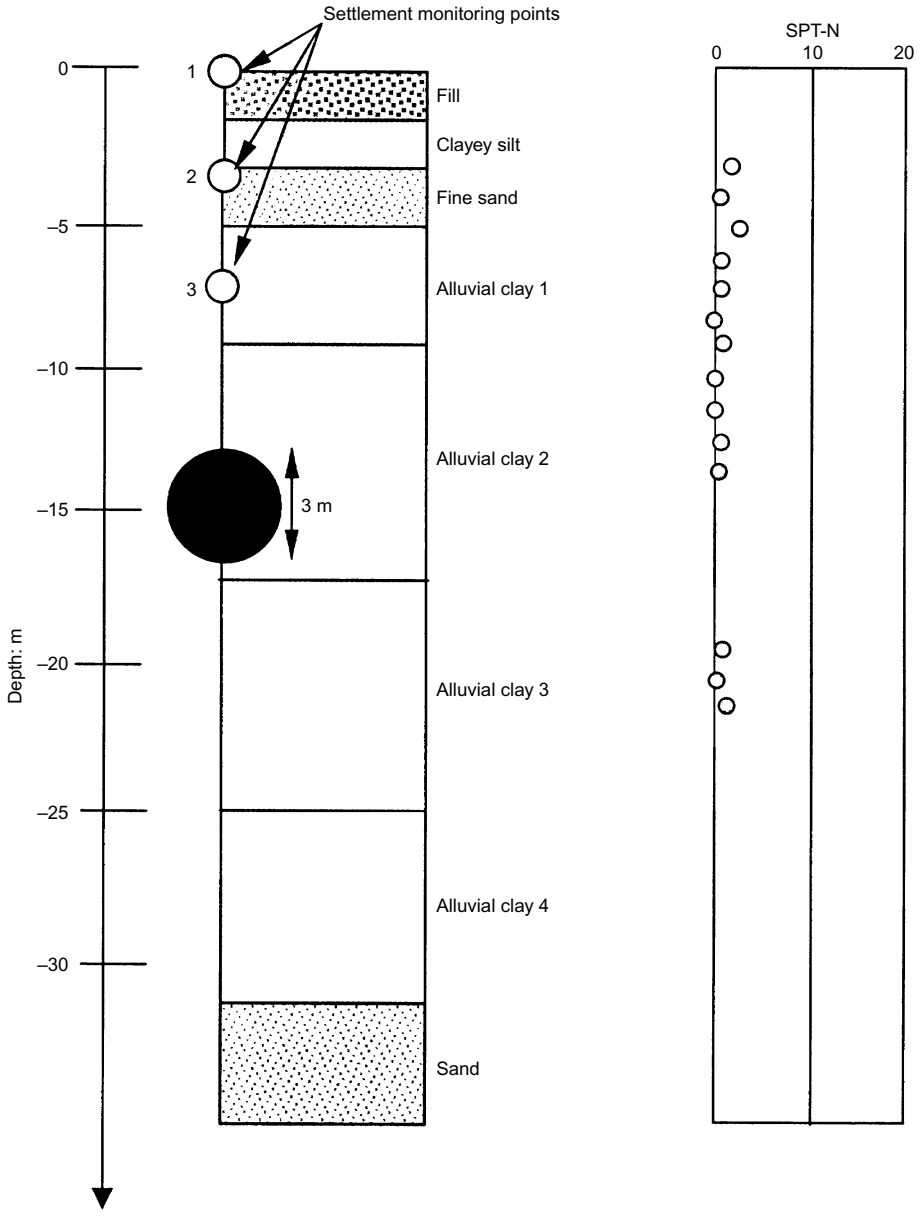


**Fig. 3. Soil profile at a field trial site**

**Table 1. Physical properties of the soils at the field trial site**

| Soil | Total unit weight, $\gamma_t$:kN/m$^3$ | Plasticity index, PI | Undrained shear strength, $q_u$:kPa | Sensitivity, $S_t$ | Void ratio, $e_0$ | Compression index, $C_c$ |
|---|---|---|---|---|---|---|
| Fill | 17 | – | – | – | – | – |
| Clayey silt | 15·6 | 23·7 | 30·9 | 10 | 1·70 | 0·94 |
| Sand | 18 | – | – | – | – | – |
| Clay 1 | 15·8 | 38·4 | 49·1 | 16 | 1·62 | 0·87 |
| Clay 2 | 15·8 | 40·4 | 66·5 | 23 | 1·56 | 0·86 |
| Clay 3 | 17·4 | 39·4 | 116 | 20 | 1·33 | 0·72 |
| Clay 4 | 17·4 | 22·2 | 143 | 41 | 1·33 | 0·49 |
| Sand | 18·0 | – | – | – | – | – |

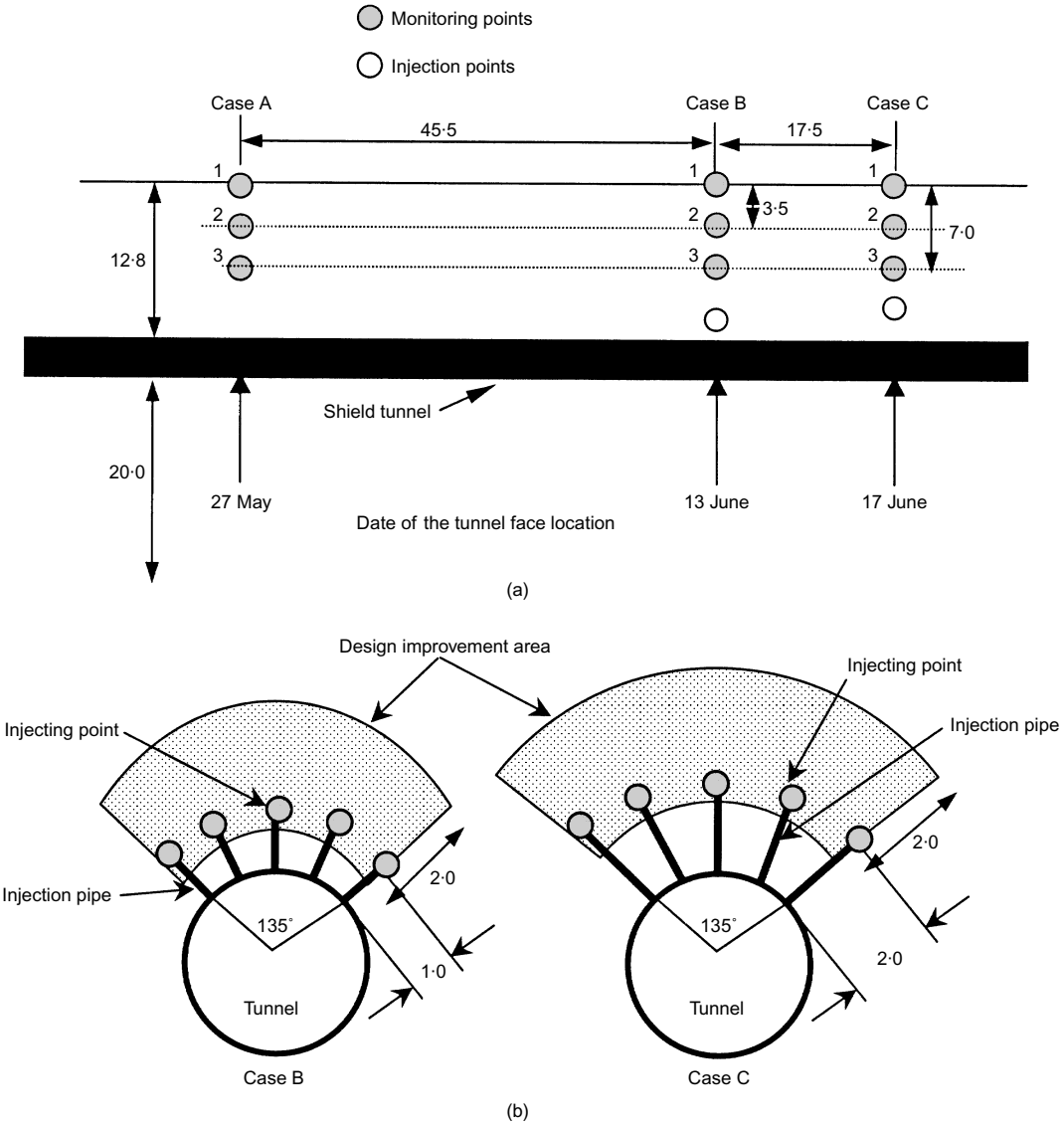


**Fig. 4. Grout injection locations: (a) side view of the tunnel and grouting locations; (b) injection details for case B and case C, dimensions in metres**

Fig. 4(b)). The ground settlement (or heave) was measured at three different locations above the injection points, as shown in Figs 3 and Fig 4(a). A mixture of cement, water and water-glass ($Na_2O$-3$SiO_2$ aq.) with gel hardening time of 20 s was used as the grout. The mass ratio of the mixture was cement : water-glass : water = 1 : 1·25 : 3·43. The use of a rapid-hardening grout was considered essential in order to avoid grout shrinkage after the injection.

The volume of injected grout was predetermined to be 3·4 m$^3$ (0·68 m$^3$ per injection tube) for case B and 6 m$^3$ (1·2 m$^3$ per injection tube) for case C. The grout was injected 8·5 h and 24 h after the machine passage in cases B and C respectively, corresponding to the time when the machine was approximately 5 m ahead of the injection points. The maximum injection pressure was recorded to be 500 kPa.

*Test results*

The measured ground displacements with time at the three monitoring locations are shown in Fig. 5, and the data are summarised in Table 2. In the table, the immediate deformations after machine passage and tail void grouting ($S_i$) and the upward displacements due to grout jacking ($S_g$) are listed (downward movement is taken as positive). The consolidation

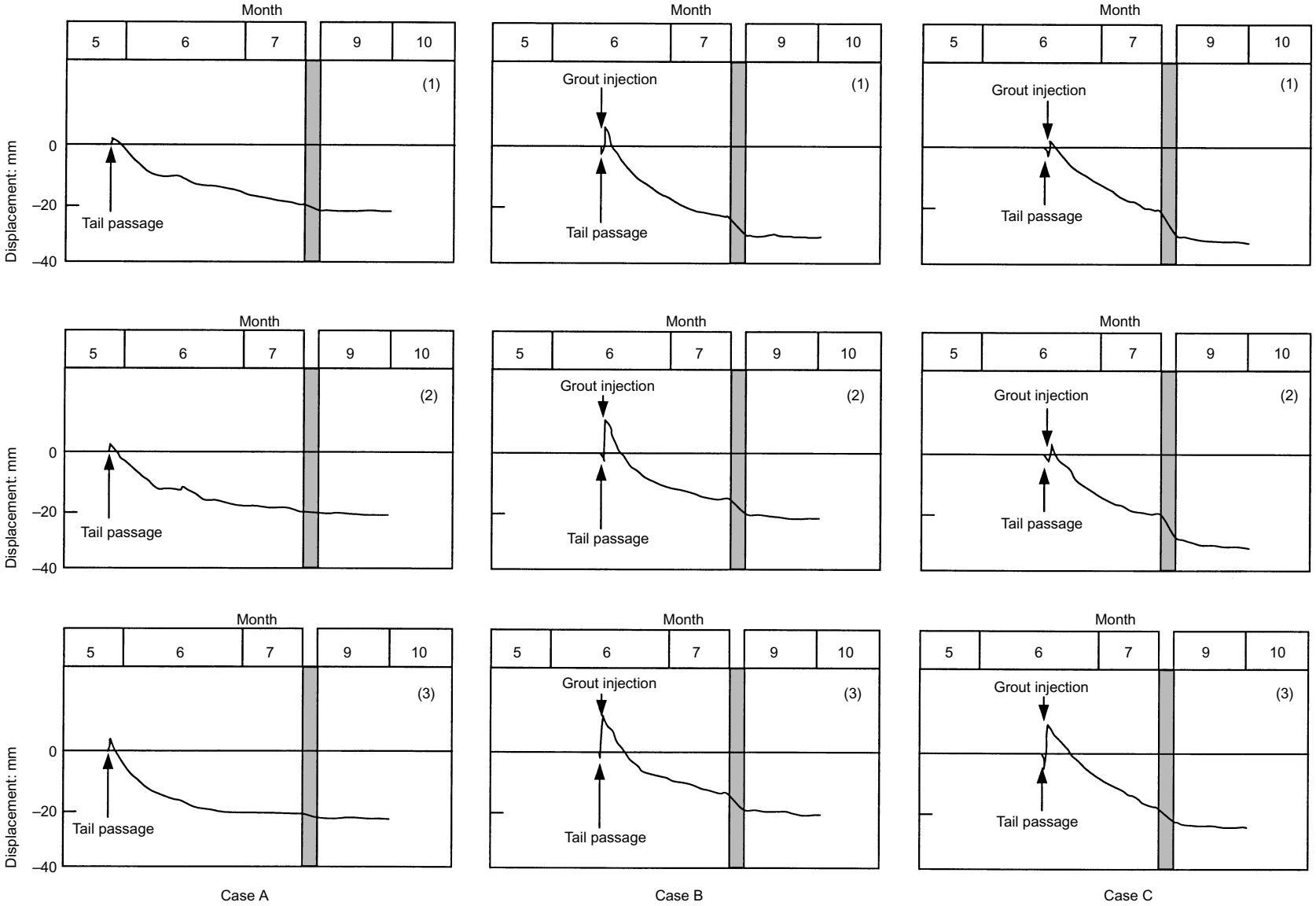


**Fig. 5. Surface/subsurface settlements at the monitoring points**

**Table 2. Summary of ground displacements from the field trial**

| Case | Monitoring point | Immediate settlement, $S_i$: mm | Heaving due to grouting, $S_g$: mm | Long-term settlement, $S_c$: mm | Final settlement, $S_f$: mm |
|---|---|---|---|---|---|
| Case A | 1 | −1·5* | – | +24·2 | +22·7 |
| | 2 | −3·0* | – | +24·0 | +21·0 |
| | 3 | −4·0* | – | +26·0 | +22·0 |
| Case B | 1 | +2·5 | −10·0 | +37·2 | +29·7 |
| | 2 | +2·5 | −14·0 | +32·8 | +21·3 |
| | 3 | +2·5 | −16·0 | +33·3 | +19·8 |
| Case C | 1 | +3·0 | −5·5 | +33·7 | +31·2 |
| | 2 | +3·0 | −7·0 | +34·5 | +30·5 |
| | 3 | +4·5 | −15·0 | +34·3 | +23·8 |

* Includes the effect of tail void grouting.

settlements ($S_c$) were measured 3 months after the grouting (at the end of month 9 in Fig. 5). The final settlement ($S_f$) is calculated as the sum of $S_i$, $S_g$ and $S_c$.

Case A showed some upward displacements immediately after tunnel construction, owing to the tail void grouting operation. The displacement decreased with increase in distance from the tunnel. The consolidation settlement, $S_c$, was smaller than the other cases, and it was approximately the same for the three measurement points (∼25 mm).

In cases B and C there were immediate settlements after machine passage owing to closure of the tail void (no tail void grouting was performed in these cases). When grout jacking was performed, the ground surface heaved more than the original level because a large amount of grout was injected. The magnitudes of the heave measured at subsurface monitoring point 3 were similar in both cases. However, a larger injection volume was required for case C to achieve this. More surface heave was obtained in case B than in case C. In case B the rigid boundary of the tunnel lining close to the injection points may have affected the soil deformation pattern. The interaction between the tunnel lining and grout injection seems to have caused more uniform upward movement of the soil above the injection points.

Both cases B and C had larger consolidation settlements, $S_c$, than case A; the jacking effect achieved in the short term disappeared. This is possibly due to additional large excess pore pressures generated when the clay was sheared and became plastic during the injection. Since the clay was sensitive and compressible, considerable consolidation settlement would occur during the dissipation of the excess pore pressures. Hence, although a good jacking effect was achieved immediately after the grout injection in this field trial, the grouting was not effective in terms of reducing the ground deformation in the long term.

## LABORATORY INVESTIGATION OF GROUTING IN CLAYS

### *Test apparatus, soils and grouts*

The field study highlighted the possible effect of soil consolidation on the long-term effectiveness of compensation grouting/grout jacking in clays. Laboratory tests were carried out by injecting two types of grouting material in three different clays: two normally consolidated clays (samples A and C), and one lightly overconsolidated clay (sample B). The tested clays were sampled from Tokyo alluvial clay deposits using either large-diameter, thin-wall sampling tubes (150 mm diameter) or block sampling. The physical properties of the clays are listed in Table 3.

A schematic diagram of the laboratory injection test apparatus is shown in Fig. 6. For the tests, cylindrical specimens of 150 mm diameter and 180 mm height were made from the tube or block samples. Before the specimen was placed into a mould, a 5 mm diameter hole was drilled from the bottom of the specimen into the centre, and an injection pipe was installed. The specimen was then consolidated from 9·8 kPa up to a specified pressure in stages. The drainage was allowed only from the top plate, and the consolidation stage took approximately one week. The final vertical pressures applied were 235 kPa for sample A specimens, 245 kPa for sample B

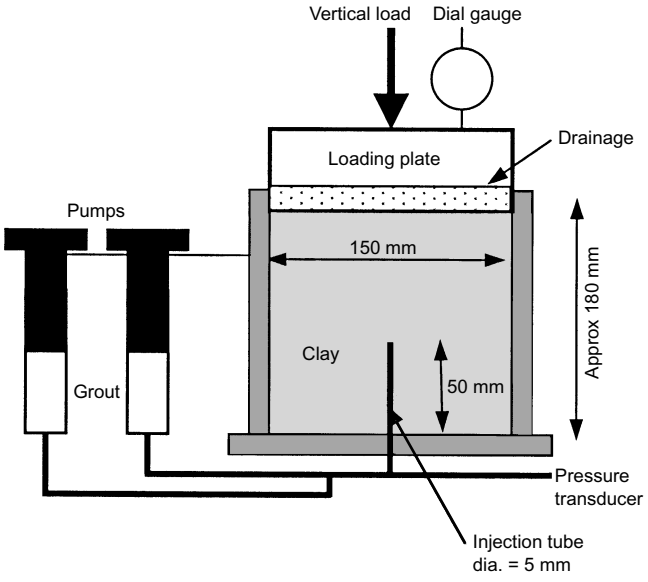


**Fig. 6. Schematic diagram of laboratory injection test**

**Table 3. Physical properties of tested clays**

| Sample | A | B | C |
|---|---|---|---|
| Name | Etchujima-clay | Yashio-clay | Keihinjima-clay |
| Water content, $w_0$ | 78% | 51% | 77% |
| Liquid limit, LL | 74% | 58% | 87% |
| Plasticity index, PI | 41% | 24% | 49% |
| Preconsolidation pressure, $\sigma_{v0}$ | 204 kPa | 392 kPa | 135 kPa |
| OCR | 1 | 1·6 | 1 |
| Undrained strength | 102 kPa | 216 kPa | 45 kPa |
| Sensitivity, $S_t$ | 17 | 14 | 8 |

specimens and 157 kPa for sample C specimens; sample A and C specimens were normally consolidated, whereas sample B specimens were overconsolidated (OCR = 1·6). After consolidation, grouting material was injected into the specimens using a manual injection pump.

Two types of grouting material were used in the experiment: (*a*) a mixture of cement and water-glass (type I), and (b) a mixture of cement, water-glass, chemical hardening material and bentonite (type II). The mass ratio of type I was cement : water-glass : water = 1 : 1·25 : 3·43. The gel-hardening time was 120 s, and its unconfined compressive strength was 75 kPa after 1 day curing. In type II, two liquids were prepared: (*a*) a mixture of water and water-glass (= 1 : 1) and (*b*) a mixture of cement, water, bentonite and chemical hardener (= 1 : 2·2 : 0·15 : 0·5). The liquids were placed in different pumps, as shown in Fig. 6, and were mixed immediately before the injection in order to avoid hardening inside the pump. With the chemical hardener, a shorter gel-hardening time of 20 s was achieved. Its unconfined compressive strength was 143 kPa after 1 day curing.

A total of 18 injection tests were performed. Type I grout was used in samples A and C and type II grout was used in samples B and C. The amount of injected grout varied between 7% and 26% of the volumes of the post-consolidated clay specimens. During injection, the injection pressure was measured by a pressure transducer connected to the injection pipe. The measured fracturing pressures were approximately 500 kPa for samples A and B and 400 kPa for sample C. The post-grout deformation was measured with time by a dial gauge placed on top of the loading plate.

In addition to the tests on natural clay specimens, the effect of grout shape (fracture or compaction type) on the long-term behaviour of soil after grouting was investigated. A rubber balloon was fitted to the injection point, and clay slurry originating from sample C (initial water content = 174%) was then poured into a mould. After consolidating the clay to a pressure of 49 kPa, the grout was injected into the balloon. The water content of the clay before injection was approximately 75%. The undrained shear strength was estimated to be 9·8 kPa from vane shear tests. It was considered that the use of a rubber balloon would prevent the grout from intruding into fractures and create a coherent grout bulb with no bleeding effect.

*Test results*

Typical cross-sectional views of grout injected specimens are shown in Fig. 7(a) and (b). In the case of small injection volume, the distribution of the grout was limited to the region adjacent to the injection point (Fig. 7(a)). The pattern of soil deformation was more or less like a compaction mode type. When more grout was injected, however, the soil fractured or deformed largely in a plastic manner, and the injected grout spread sideways to form a horizontal layer (Fig. 7(b)).

In all cases the top loading plate displaced upwards immediately after the injection as the clay heaved. The amount of volume expansion calculated from the initial displacement of the top plate was approximately equal to the injection volume, indicating that the soil deformation during injection was in the undrained condition. The vertical displacement of the top plate was continuously measured for several days until the excess pore pressure in the specimen had dissipated and the rate of settlement became negligible.

The upward displacement of the top plate was plotted against the normalised injection volume (grout volume/initial soil volume), as shown in Fig. 8. For each test, two data points are plotted: the upper value is the heave immediately after injection, whereas the lower value is the final heave after excess pore pressure dissipation. The decrease in the heave with time is due to (*a*) dissipation of the excess pore pressures in the clay generated during grout injection and (*b*) shrinkage of the grout itself by 'bleeding' its water into the surrounding soil. When a faster-setting grout was used, the long-term settlement was smaller because of reduced grout shrinkage.

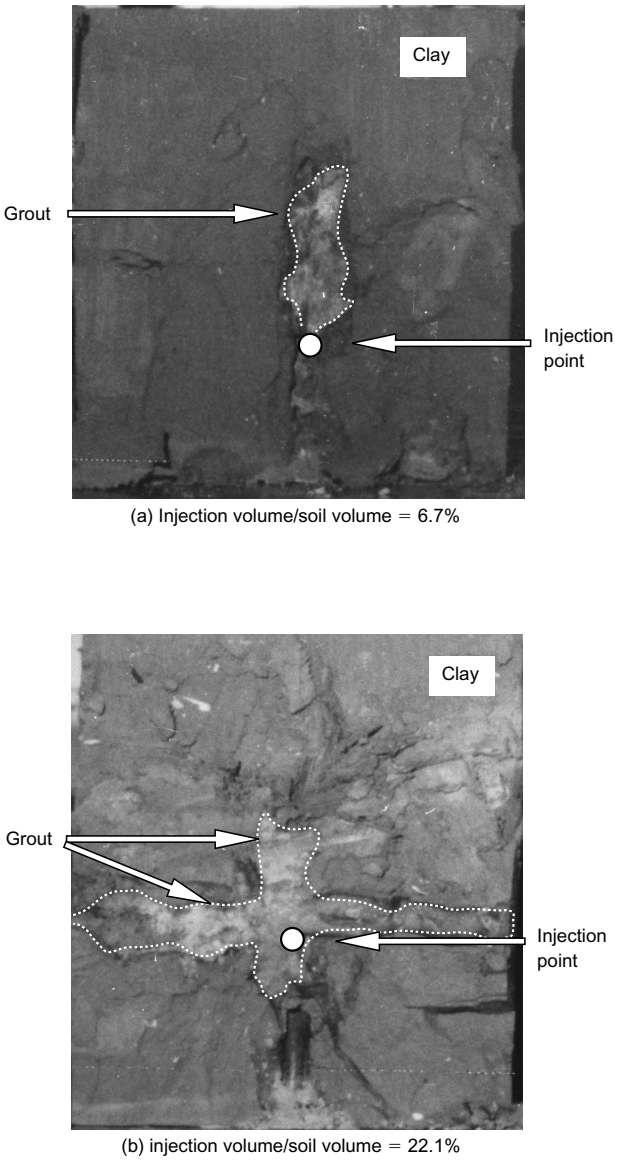


**Fig. 7. Photos of sample after grout injection (sample A): injection volume/soil volume (a) 6·7%, (b) 22·1%**

In this paper the grout efficiency, $\eta_{lab}$, measured in the laboratory is defined as follows:

$$\eta_{lab} = \frac{\text{Heaved volume } (V_f)}{\text{Injection volume } (V_i)} = \frac{V_i - V_c - V_G}{V_i} = 1 - \lambda_C - \lambda_G \quad (1)$$

where $V_i$ is the injection volume, $V_C$ is the decrease in volume due to consolidation, and $V_G$ is the decrease in volume due to grout bleeding. The volume loss ratios of consolidation effect and grout bleeding are defined as $\lambda_C = V_C/V_i$ and $\lambda_G = V_G/V_i$ respectively.

Typical curves of grout efficiency against time are shown in Fig. 9. Immediately after injection the grout efficiency is close to 1, but it reduced with time. For example, when a small volume of grout (injection volume/soil volume = 6·7%) was injected in sample A, the grout efficiency reduced to less than 10% after 1 day. The grout efficiency of sample A increased to 60% as the injection volume increased (injection volume/soil volume = 22·1%). Better grout efficiency was obtained when the fast-setting type II grout was used.

In order to separate the soil consolidation effect from the bleeding effect, $\lambda_G$ in equation (1) needs to be determined.

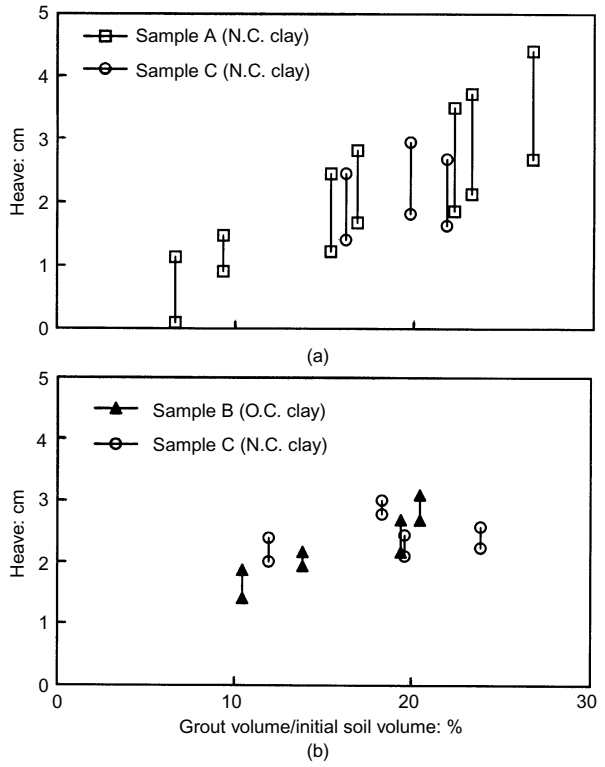


**Fig. 8. Measured initial and final heaves of the upper plate: (a) type I grout; (b) type II grout**

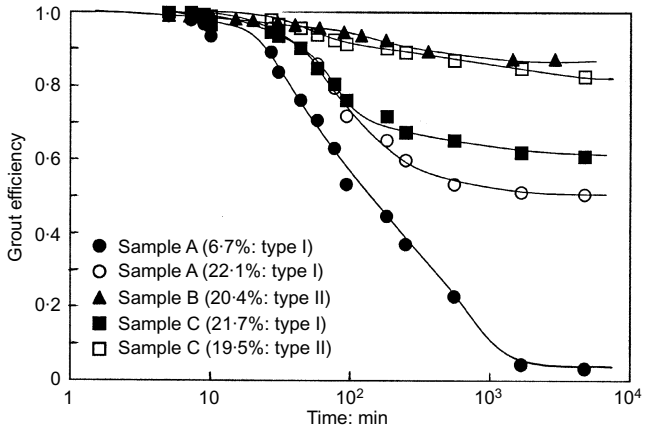


**Fig. 9. Changes in grout efficiency with time**

Consolidation tests were performed on the tested grouts with the same consolidation mould as used for the grouting tests. The grout was placed between two clay blocks, and a vertical stress corresponding to the injection tests was applied. Type I grout after hardening lost 30% of its original volume ($\lambda_G = 0{\cdot}30$), whereas, for type II grout, $\lambda_G$ reduced to 0·07. Although it is possible that more bleeding will occur in the injection tests owing to larger injection pressure, these values were used as the volume loss due to grout bleeding ($\lambda_G$) for the subsequent discussion. However, further investigation on the compressibility of grout is needed for better characterisation of the tested grouts.

Using equation (1) with measured $\eta_{lab}$ and $\lambda_G$, the implied volume loss due to consolidation ($\lambda_C$) can be estimated. The calculated values of $\lambda_C$ for different injection volumes are shown in Fig. 10. For small injection volumes, there is a large loss due to soil consolidation ($\lambda_C = 0{\cdot}65$): the grout efficiency is therefore small owing to excess pore pressure development during injection and subsequent consolidation of the clay. As

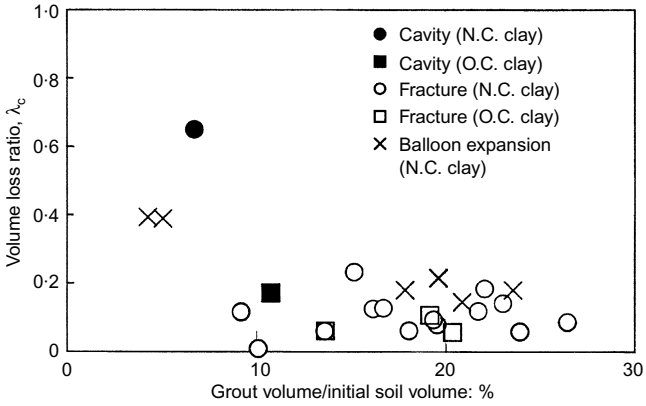


**Fig. 10. Volume loss ratio due to consolidation**

the injection volume increased, $\lambda_C$ decreased to a value of approximately 0·10, and consequently the grout efficiency increased. The calculated volume loss ratio, $\lambda_C$, was independent of the type of grout used, suggesting that the pattern and amount of excess pore pressure development during injection were similar for both type I and II grouts.

As shown in Fig. 10, the overconsolidated clay (sample B) had a smaller volume loss than the normally consolidated clays (sample A) when the grout formed a bulb (solid symbols). This is due to the smaller excess pore pressures developed and the smaller plastic zone generated for a given injection volume compared with the normally consolidated clay.

The pattern of volume loss obtained from the grout injection into a balloon (cross symbols in Fig. 10) was similar to that without the balloon: $\lambda_C$ decreased with increasing injection volume. The difference in volume loss between the balloon cases and the grout injection cases was approximately 0·1. The difference may be due to the mode of soil deformation (cavity mode rather than fracture mode) and variation in the initial conditions (natural rather than reconstituted specimens, applied vertical stresses, etc.). It was also considered that the size (or the boundary) of the mould might have affected the deformation pattern of the soil around the grout, and hence the grout efficiency. This boundary effect will be investigated in the numerical analysis described in the next section.

The boundary condition imposed in the laboratory tests needs extra consideration for any practical implications of the findings for a field scenario. In the laboratory tests, the grout cannot escape laterally because of the mould boundary; it is contained in the mould. In the field, the grout can escape laterally to any extent from the designed area. This will result in decreasing grout efficiency, especially when low-viscosity grout is used: hence the small volume losses at large injection volumes measured in the laboratory may not occur in the field.

## FINITE ELEMENT MODELLING OF GROUTING IN CLAYS

### *Simulation of the laboratory experiments*

Compensation grouting or grout jacking in the field involves a series of complex procedures and stages (for example drilling the borehole, installing tubes-a-manchettes, filling the borehole with cement bentonite, and pre-conditioning). Obviously some of these procedures are very complicated, and it is very difficult to model all the stages in great detail. However, the laboratory investigation described above highlighted the effect of the overconsolidation of clay and the boundary condition on the long-term grout efficiency. An attempt was made here to assess the finite element method's ability to model the long-term behaviour of grouting observed in the laboratory.

Several assumptions were made in the numerical investigation in order to capture the most important features of compensation grouting responsible for its long-term effectiveness. The finite element mesh used to model the laboratory tests is shown

in Fig. 11. The model geometry is the same as in the laboratory tests. The wall friction was assumed to be zero. The initial size of injection cavity was taken to be equal to the size of the injection needle diameter. Four-node axisymmetric consolidation elements (Akai & Tamura, 1978) were adopted for the analysis. The Cam-clay model (Schofield & Wroth, 1968) was used, and the material properties and the initial conditions are listed in Table 4.

At the beginning of the analysis, the initial condition of the sample (stress state and stress history) was defined. The grout injection process was simulated by applying uniform pressure at the boundary of the injection cavity; the fracturing phenomenon is not simulated. The pressure was ramped until a specific injection volume was obtained. After fixing the nodes at the cavity boundary, consolidation analysis was then performed until the excess pore pressures in the model became zero. The injection volume is fixed throughout the consolidation analysis, which means that bleeding of the grout is not modelled. The displacement of the top boundary was computed with time to calculate the volume loss ratio, $\lambda_C$. As the cavity boundary is fixed, $\lambda_G$ is equal to zero in the analysis.

The volume loss ratio was computed from various injection volumes for both the normally consolidated condition (sample A) and the overconsolidated condition (sample B). As shown in Fig. 12, a trend similar to that found in the laboratory tests was obtained. Smaller volume loss ratios were obtained for the overconsolidated condition than for the normally consolidated condition, and the volume loss ratio decreased with increasing injection volume. The computed volume loss at large injection volume was close to the results of the balloon tests.

The contours of the excess pore pressures developed immediately after grout injection are shown in Fig. 13 for three different injection volumes (5%, 11% and 23% of the original soil volume) in sample A. In the figure, the calculated excess pore pressures were normalised by the maximum excess pore pressure. It is clear that the mould boundary starts to affect the pattern of excess pore pressures in the specimen as the injection volume increases. The location of the maximum excess pore pressure moves from the injection boundary into the soil. Moreover, the actual magnitudes of the excess pore pressures do not increase as much as the increase in the injection pressure or volume. This is the main reason why the volume loss due to consolidation is small in the large injection volume cases. It seems that the change from cavity expansion to fracture observed in the laboratory had only a small influence in increasing the grout efficiency.

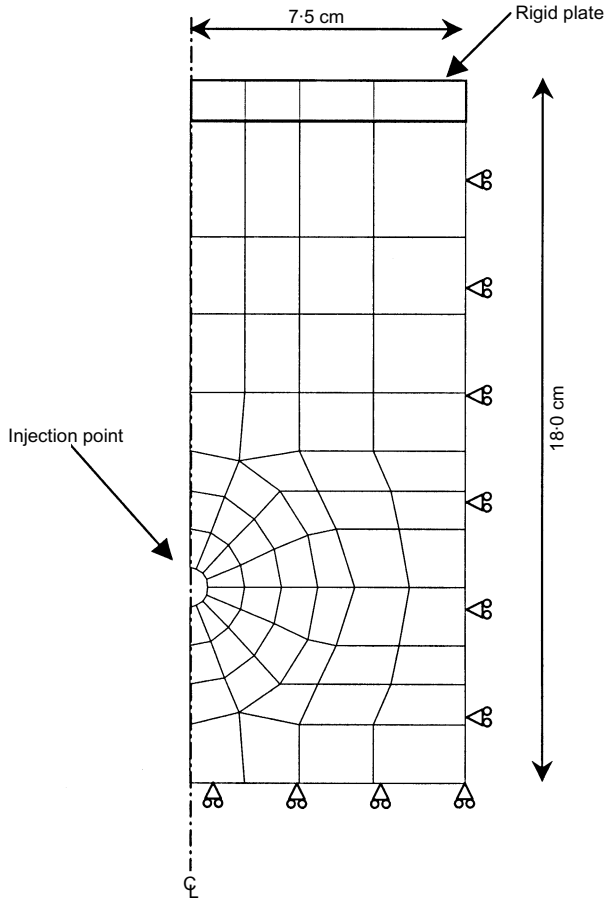


**Fig. 11. FE mesh used for laboratory simulation**

*Simulation of the field trial*

Both laboratory tests and the finite element analysis showed that soil consolidation due to the excess pore pressure generated during grout injection was responsible for reducing the grout efficiency in the long term, especially for normally consolidated clay. The finite element analysis of the laboratory tests highlighted the importance of the boundary effect when long-term grout efficiency needs to be assessed. Therefore the grout–soil interaction needs to be solved as a boundary value problem. Adopting the same modelling technique used to simulate the laboratory tests, the field trial described earlier was simulated.

The three-dimensional finite element mesh used for the analysis is shown in Fig. 14. The mesh models both case B and case C conditions. A total of 11 232 eight-noded cubic

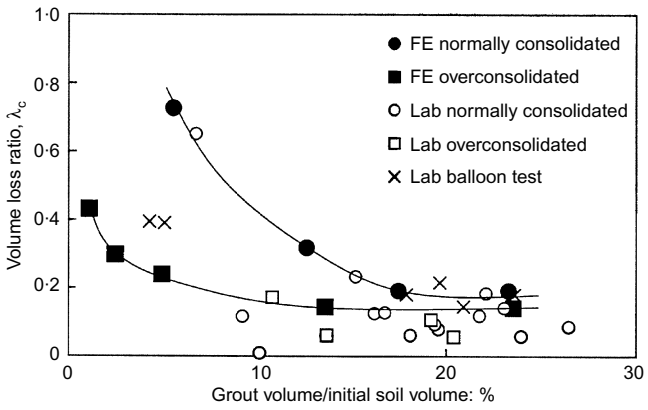


**Fig. 12. Finite element results of volume loss ratio due to consolidation**

**Table 4. Cam-clay properties used for simulation of the laboratory experiment**

| Name | Normally consolidated clay | Overconsolidated clay |
|---|---|---|
| | Sample A | Sample B |
| $\lambda$ | 0·647 | 0·23 |
| $\kappa$ | 0·107 | 0·038 |
| $M$ | 1·02 | 1·17 |
| $e_0$ at 1 kPa | 1·8 | 1·25 |
| Poisson's ratio, $\nu$ | 0·361 | 0·338 |
| $p_0$ | 235 kPa | 402 kPa |

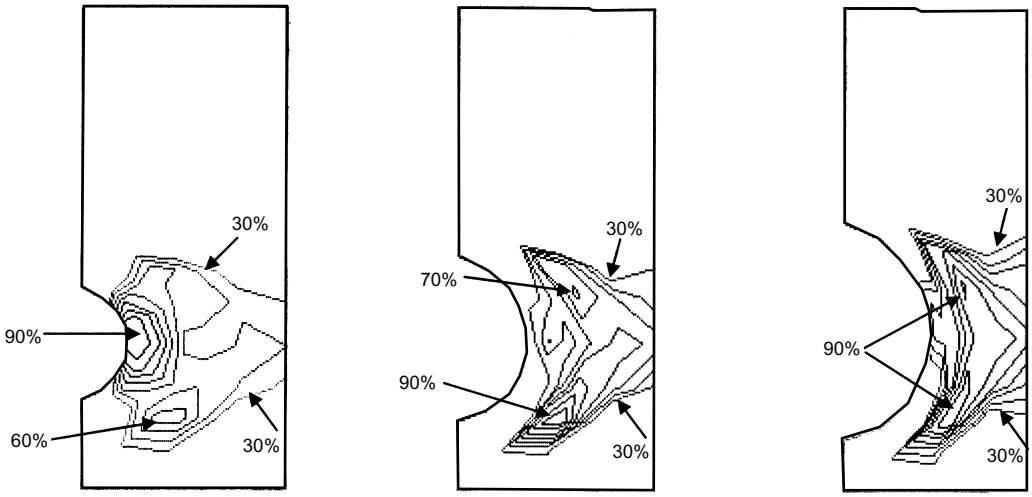


| | | | |
|---|---|---|---|
| Injection volume/ initial soil volume | 5% | 11% | 23% |
| Injection pressure | 496 kPa | 600 kPa | 704 kPa |
| Maximum excess pore pressure | 166 kPa | 197 kPa | 226 kPa |

**Fig. 13. Computed excess pore pressure development during injection; normalised excess pore pressure contours (= excess pore pressure/maximum excess pore pressure) increment of 10% from 30%**

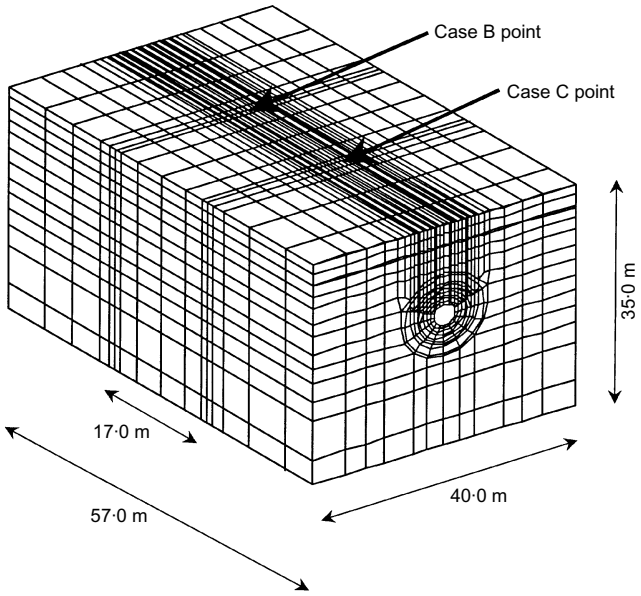


**Fig. 14. FE mesh of field trial**

consolidation elements were used to model the soil. The Cam-clay material properties were determined independently from conventional laboratory tests, and they are listed in Table 5. The tunnel lining was modelled using rigid beam elements, and the tunnel boundary was assumed to offer no drainage.

The injection points were modelled as an initial cavity size of 0·07 m diameter, which is the same as the injection pipe diameter. As in the laboratory test simulation, the grout injection was modelled by applying uniform pressure at the cavities. The magnitude of the applied pressure was increased until the computed heave at monitoring point 3 matched the measured one. The cavity boundaries were then fixed, and consolidation analysis was performed. It is important to note here that the construction of a tunnel is not modelled in this analysis. The geometry of the tunnel is fixed, and there is no inward movement of the soil into the tunnel: hence the computed deformation will be due to grouting operation only. The analysis was intended to investigate the long-term effect of grout jacking decoupled from the effect of tunnel construction.

**Table 5. Material properties used for simulation of the field trial**

| | Layer | | |
|---|---|---|---|
| | 1 | 2 | 3 |
| Depth | 0–10 m | 10–15 m | Below 15 m |
| $\lambda$ | 0·291 | 0·371 | 0·311 |
| $\kappa$ | 0·049 | 0·062 | 0·052 |
| $M$ | 1·04 | 1·02 | 1·03 |
| $e_0$ at 1 kPa | 1·62 | 1·56 | 1·33 |
| $\nu$ | 0·358 | 0·361 | 0·360 |
| $K_0$ | 0·558 | 0·565 | 0·562 |
| $k$ | $10^{-9}$ m/s | $10^{-9}$ m/s | $10^{-9}$ m/s |

In order to match the heave at monitoring point 3, the volume expansion necessary for each injection point was only 0·007 23 $m^3$ and 0·005 12 $m^3$ for cases B and C respectively. These values are much smaller than the actual injected volumes (0·68 $m^3$ and 1·2 $m^3$ for cases B and C respectively). In the field, the other portion of the low-viscosity grout may have escaped into the fractures formed during injection. Unfortunately, no field inspection was conducted to confirm this.

The computed deformations with time at the three monitoring points are compared with the measured data in Figs 15 and 16 for cases B and C respectively. The computed heaves at monitoring points 1 and 2 immediately after the injection agreed reasonably well with the actual measurements. The initial heave achieved by grout jacking gradually decreased with time as the excess pore pressures generated by the cavity expansion dissipated. The final settlements were greater than the heave initially generated. The large injection pressures at the injection points sheared the surrounding normally consolidated clay, and large excess pore pressures were generated, leading to large consolidation settlements during the dissipation.

Although the trends are similar, the computed long-term displacements are smaller than the measured ones: the difference is approximately 10 to 15 mm. It is considered that this

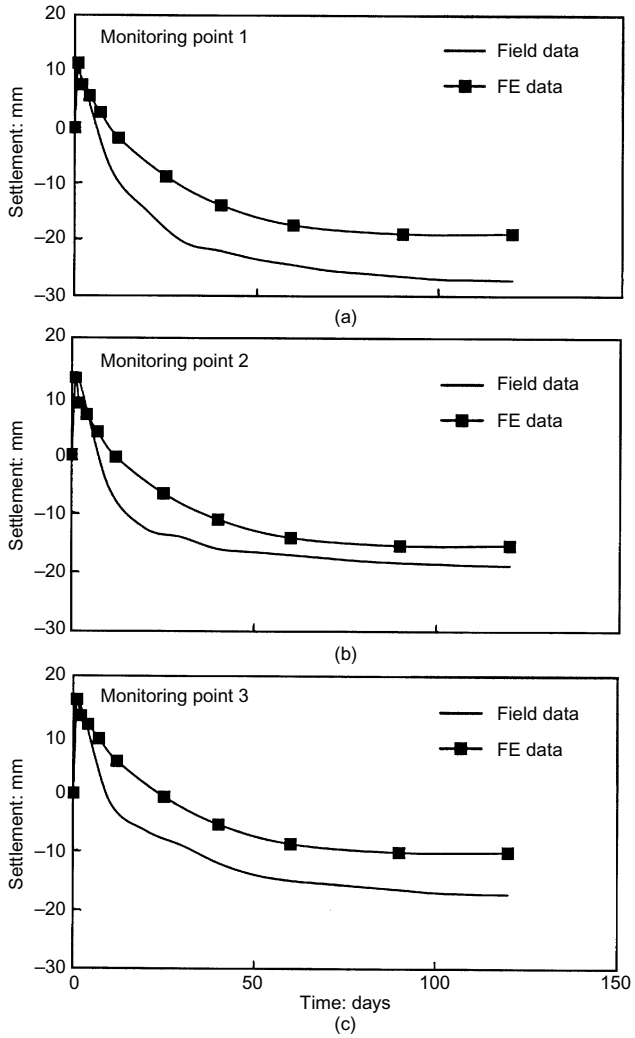


**Fig. 15. Comparison between computed results and field data for case B**

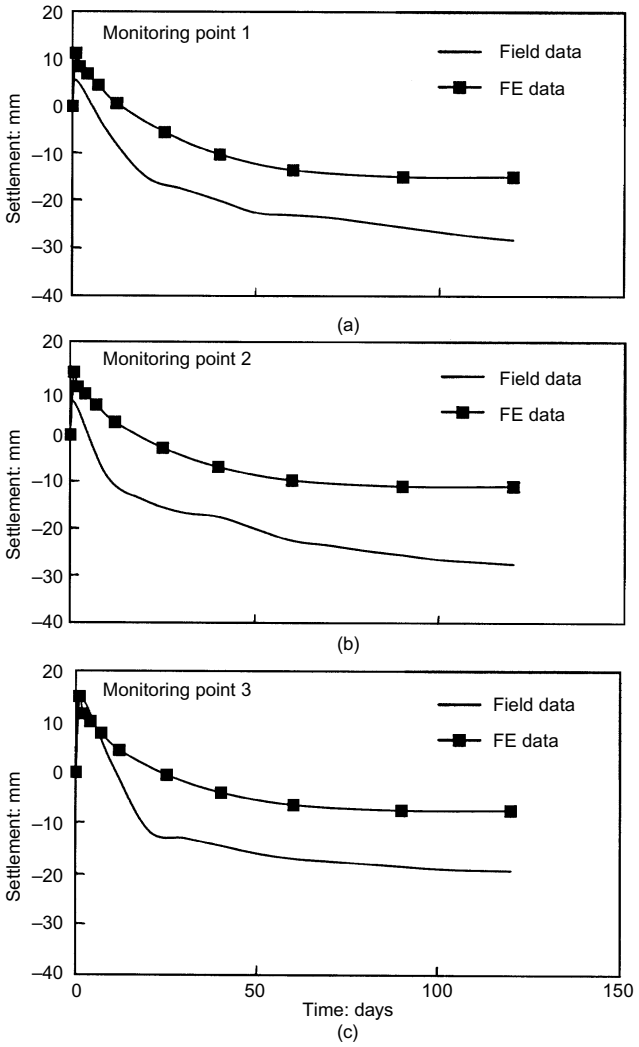


**Fig. 16. Comparison between computed results and field data for case C**

discrepancy is due mainly to the additional excess pore pressures generated during the shield tunnel construction and the change in drainage condition around the tunnel, which will also contribute to the long-term deformation of the surrounding soil.

Case A was also simulated by expanding the tunnel boundary radially until the computed displacement at monitoring point 3 matched the actual one. Fig. 17 shows the computed settlement curves compared with the long-term measurements at the three monitoring points. Again, the measured settlements are approximately 10–15 mm larger than the computed ones, which is similar to the results found in cases B and C. Therefore, in order to match the actual measurements, the shield machine excavation process needs to be modelled.

## CONCLUSIONS

The effectiveness of grout jacking to reduce surface settlements during underground construction in clayey ground was investigated by a field trial in Tokyo. The results from the field trial showed that, although sufficient heave was achieved immediately after the grout injection, the ground continued to settle with time owing to grout shrinkage and soil consolidation associated with the excess pore pressures developed during the grout injection. Larger long-term ground settlements were observed in the grout jacking operation compared with the tail void grouting operation.

A laboratory investigation was conducted to find the parameters that reduce the long-term grouting efficiency in clays. It was found that better long-term grouting efficiency can be achieved in overconsolidated clays than in normally consolidated clays, and the efficiency increased with increasing injection volume. Finite element analysis of the laboratory experiments confirmed that the amount and extent of excess pore pressures generated during injection govern the long-term grout efficiency. When the soil deformed as an expanding cavity, the grout efficiency was as low as 10%. However, when a large amount of grout was injected, the grout efficiency increased as the clay fractured and the grout penetrated into the fractures. The finite element analysis of the laboratory tests confirmed that the mould boundary contributed to the increase in the grout efficiency.

Finite element analysis of the field trial was performed to simulate the long-term ground deformation after grout injection. Adopting the same modelling technique as used in the laboratory test simulation, it was possible to obtain a similar trend for the long-term behaviour of grout jacking as observed in the field trial. The final settlements were greater than the initial heave generated, owing to the large excess pore pressure generated in the sensitive clay around the injection points. However, the actual shield tunnel construction process needs to be modelled in order to match the field data.

## ACKNOWLEDGEMENT

The authors would like to acknowledge the financial support from the Brite Euram programme of the European Commission.

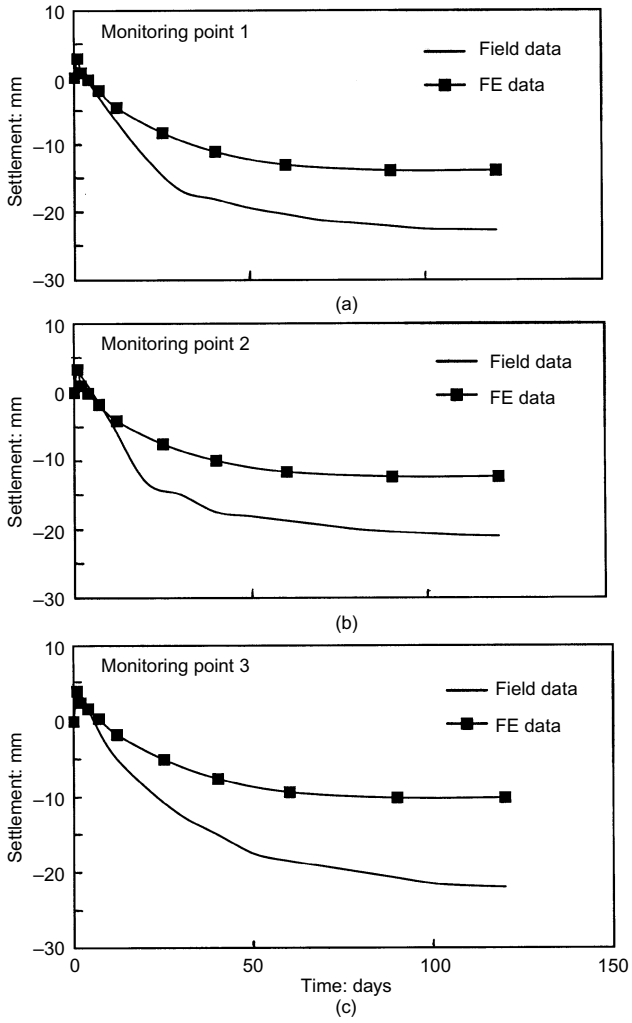


**Fig. 17. Comparison between computed results and field data for case A**

REFERENCES

Akai, K. & Tamura, T. (1978). Numerical simulations of multiple dimensional consolidation caused by elasto-plastic constitutive equation. *J. Geotech. Engng*, *Japan. Soc. Civ. Engrs*, No. 269, 95–104 (in Japanese).

Clough, G. W., Sweeny, B. P. & Finno, R. J. (1983). Measured soil response to EPB shield tunnelling. *J. Geotech. Engng, ASCE* **109**, No. 2, 131–149

Harris, D. I., Pooly, A. J., Menkiti, C. O. & Stephenson, J. A. (1996). Construction of low-level tunnels below Waterloo Station with compensation grouting for the Jubilee line. In *Geotechnical aspects of underground structures* (eds R. J. Mair and R. N. Taylor), pp. 361–366. Rotterdam: Balkema.

Harris, D. I., Mair, R. J., Burland, J. B. & Standing, J. A. (1999). (eds Kusakabe, Fujita and Miyazaki) Compensation grouting to control tilt of Big Ben clock tower. In *Geotechnical aspects of underground construction in soft ground*. (IS-Tokyo 99), pp. 225–232 Rotterdam: Balkema.

JSSMFE (1993). *Underground construction in soft ground in Japan*. JSSMFE (Japanese Society of Soil Mechanics and Foundation Engineering) Committee on Underground Construction in Soft Ground, Tokyo.

Mair, R. J. & Hight, D. W. (1994). Compensation grouting. *World Tunnelling*, Nov., 361–367.

Mair, R. J. & Taylor, R. N. (1997). Bored tunnelling in the urban environment. *Proc. 14th Int. Conf. Soil Mech. Found. Engng*, **4**, Hamburg 2353–2385.

Mori, A. and Akagi, H. (1985). Effect of backfilling at shield work in soft cohesive soil. *Proc. 11th Int. Conf. Soil Mech. Found. Engng*, **4**, San Francisco 1667–1670.

Mori, A., Tamura, M. & Fukui, Y. (1990). Fracturing pressure of soil ground by viscous materials. *Soils Found.* **30**, No. 3, 129–136.

Mori, A., Tamura, M., Shibata, H. & Hayashi, H. (1992). Some factors related to injected shape in grouting. *ASCE Proc. Grouting, Soil Improvement and Geosynthetics, New Orleans*, pp. 313–324.

Osborne, N., Murry, K., Chegini, A. & Harris, D. I. (1997). Construction of Waterloo Station upper level tunnels, Jubilee line extension project. *Proc. Tunnelling 97*, pp. 639–662. London: Institution of Mining and Metallurgy.

Schofield, A. N. & Wroth, C. P. (1968). *Critical state soil mechanics*. London, McGraw-Hill.

Shirlaw, J. N. (1995). Observed and calculated pore pressures and deformations induced by an earth pressure balance shield: Discussion. *Can. Geotech. J.* **32**, 181–189.

Shirlaw, J. N., Dazhi, W., Geneshan, V. & Hoe, C. W. (1999). A compensation grouting trail in Singapore marine clay. (eds Kusakabe, Fujita and Miyazaki) In *Geotechnical aspects of underground construction in soft ground*. (IS-Tokyo 99) pp. 149–154 Rotterdam: Balkema.

Soga, K., Bolton, M. D., Au, S. K. A., Komiya, K., Hamelin, J. P., Van Cotthem, A., Buchet, G. & Michel, J. P. (2000). (eds Kusakabe, Fujita and Miyazaki) Development of compensation grouting modelling and control system. In *Geotechnical aspects of underground construction in soft ground*. (IS-Tokyo 99) pp. 425–430 Rotterdam: Balkema.

Warner, J. (1992). Compaction grouting: rheology vs. effectiveness. *ASCE Proc. on Grouting, Soil Improvement and Geosynthetics, New Orleans*, **2**, No. 1, pp. 694–707

Warner, J. (1998). Pressure behaviour: an important monitoring tool in grouting. *Ground Improvement*, No. 2, 5–10.